Supporting Information

Ultrafast Broadband Spectroscopy of Widely Spread Excitonic Features in WSe_2 Nanosheets

Tanmay Goswami[†], Himanshu Bhatt[†], Dharmendra Kumar Yadav[†], Hirendra N. Ghosh[‡, *]

[†]Institute of Nano Science and Technology, Knowledge City, Sector 81, SAS Nagar, Punjab-140306, India

[‡] School of Chemical Sciences, National Institute of Science Education and Research (NISER), Bhubaneswar, Odisha 752050, India

*E-mail: hnghosh@niser.ac.in, hnghosh2004@gmail.com

Materials used for synthesis of WSe_2 NSs

Tungsten hexacarbonyl ($W(CO)_6$), selenium (Se), trioctylphosphine oxide (TOPO), Squalene, oleic acid and oleylamine were purchased from Sigma Aldrich, India. Analytical grade methanol and toluene were used as received without further purification. The selenium stock solution was prepared by dissolving 0.28 mmol of selenium powder in 2 ml of oleylamine at 300°C under nitrogen atmosphere.

Synthesis procedure

The WSe_2 NSs were prepared via solution phase hot injection synthetic approach. To start with, 0.1 mmol tungsten carbonyl, 0.4 mL oleic acid, 2.4 mL oleylamine, 2.0 g trioctylphosphine oxide, and 4.0 mL squalene were mixed into a three-neck flask under vacuum for 30 min. Further, the mixture was heated to 140°C followed by degassing for 30 min to remove the water and other impurities. The solution colour changed from greenish to dark reddish yellow in that process. After that, the solution was gradually heated to 330°C in inert condition (N_2 atmosphere), when the colour of the solution was changed into light yellow. Then, selenium precursor (0.28 mmol in 2 mL oleylamine) was injected at once in the reaction mixture. Following injection, the solution colour was instantly turned black colour, indicating growth of the WSe_2. This mixture was kept at 330°C for 1h. After that, the reaction was naturally cooled down up to 80°C. At this point 8 mL toluene was injected in the reaction mixture in order avoid any precipitation of unreacted TOPO and oleate ligands. The WSe_2 NSs was precipitated by using methanol. The product solution was centrifuged at 5000 rpm for 10 min and washed several times with toluene and methanol. Finally, a black colour precipitate was obtained and dispersed in toluene for further characterization.

Material Characterisation

As prepared WSe_2 sheets were characterised using XRD, Raman, AFM, TEM and UV-VIS Absorption spectroscopic measurements. The BRUKER D8 ADVANCE with Cu-Kα radiation (λ = 1.542 Å) was used to carry out the powder-XRD measurements. Raman spectra were collected with a 532 nm laser line using a WITEC alpha 300 R Raman spectrometer. A Bruker Multimode 8 AFM system was used for AFM imaging of WS_2 flakes in tapping mode under ambient conditions. The morphological features of the WSe_2 layers were obtained using Transmission Electron Microscope (TEM, JEOL JEM 2100) at an accelerating voltage of 200 kV. The steady-state absorption spectra of the synthesized samples were recorded using a Shimadzu UV-2600 UV-vis spectrophotometer.

Femtosecond transient absorption spectroscopy

The ultrafast setup was comprised of a Ti: sapphire amplifier system (Astrella, Coherent, 800 nm, 3mJ/pulse energy, ~ 35 fs pulse width and 1 kHz repetition rate) and Helios Fire pump-probe spectrometer.[48] With the help of two beam splitters the output laser pulses were cleaved into pump (95% of the output) and probe (remaining 5%) beams. Optical Parametric Amplifier (OPerA-SOLO) was in place of pump beam to produce required wavelength for the photoexcitation of the sample. A delay stage is operating in path of probe beam to maintain a perfect delay between pump and probe in temporal sense throughout the experimental procedure. Monochromatic probe light passes through a CaF_2 crystal generating UV-Visible probe pulses. Probe beam passes through sample dispersion and falls upon fibre coupled CMOS detectors connected with the computer system. WS_2 few layer solutions in a 2 mm quartz cuvette were taken as sample. All the experimental measurements were carried out at room temperature. The collected TA data were chirped and fitted multi-exponentially using surface explorer software.

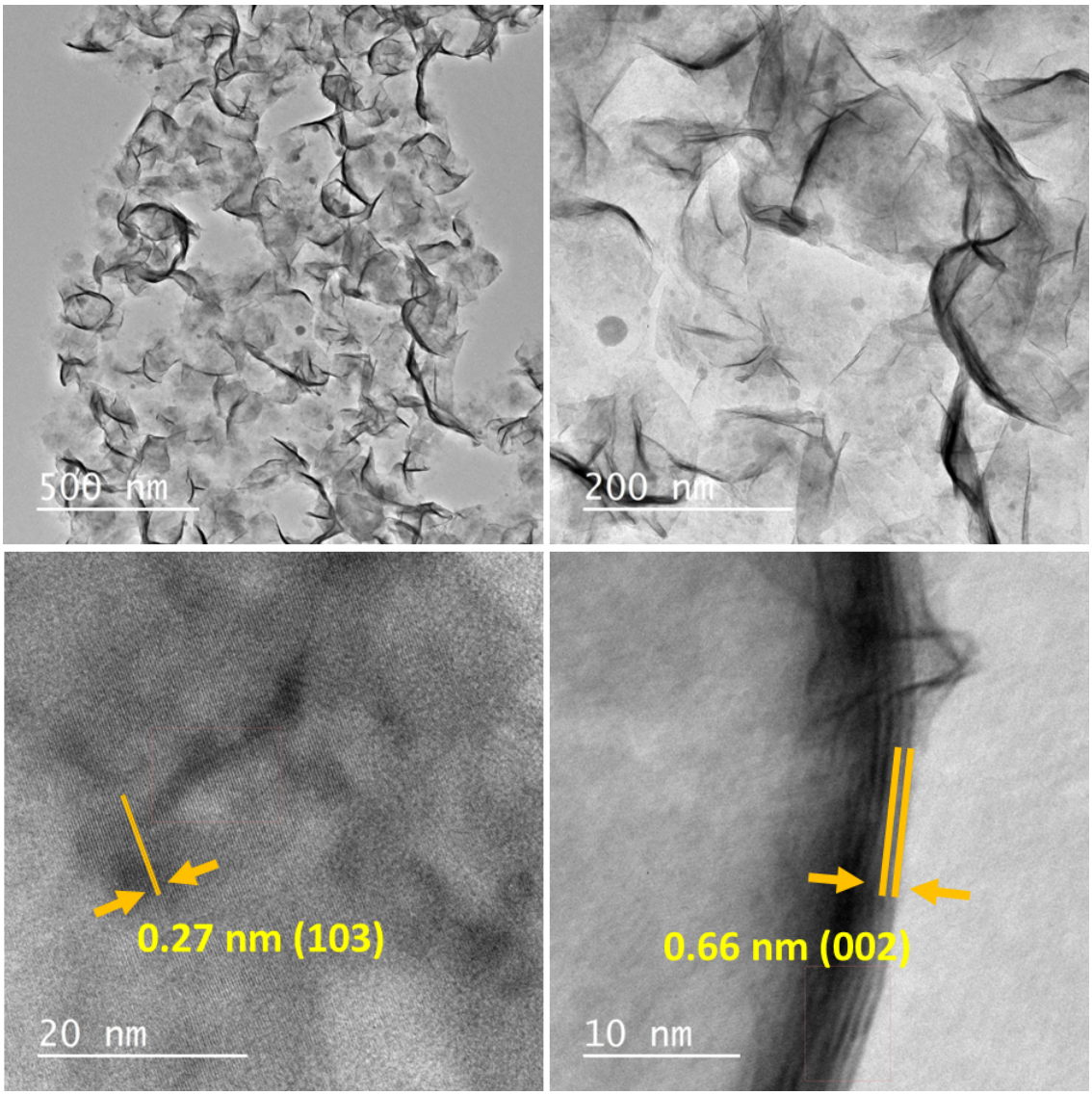

Figure S1: TEM and HRTEM images of WSe_2 nanosheets representing (100) and (002) planes of WSe_2.

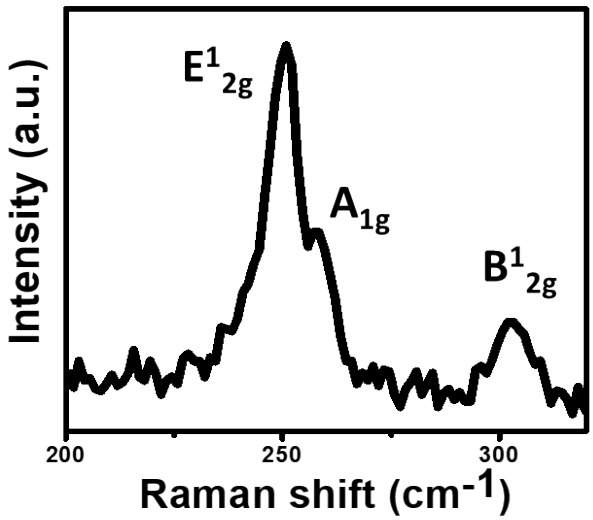

Figure S2: Room temperature Raman spectra of WSe_2 NSs following 532 nm laser excitations.

Raman spectroscopy is a powerful tool to characterize the layered TMDCs material. It provides valuable information on layer number, strain, interlayer interaction and various phonon interactions. The Raman spectra of TMDC materials are usually dominated by two vibration modes: E^1_{2g} and A_{1g}. In the present work, we also recorded the Raman spectra of colloidal WSe_2 after the excitation of the 532 nm laser, as shown in Figure 2d and S2. The spectrum is composed of two closely spaced peaks around 250.2 and 259.7 cm-1, which corresponds to the E^1_{2g} and A_{1g} vibrational modes of WSe_2. The E^1_{2g} mode originates from the in-plane opposite direction oscillation of W and Se atoms, whereas the out-of-plane vibration of Se atoms results in A_{1g} mode. The peak difference and intensity ratio of E^1_{2g} and A_{1g} modes were found to be 9.5 cm-1 and 0.3 (A_{1g} / E^1_{2g}), respectively. These values strengthen the possibility of few-layered WSe_2 formation, though exact layer numbers cannot be extrapolated, unlike MoS_2, WS_2, etc. The wavenumber difference and intensity ratio between both peaks (E^1_{2g} and A_{1g}) have already been correlated with the layer number in the TMDCs.[1–4] Zeng et al. investigated the change in these parameters for tungsten dichalcogenides (WS2 and WSe2) with an increasing number of monolayers.[1] The Raman spectrum also represents a distant peak at 302.7 cm-1 (B^1_{2g}), as shown in Figure S2, which stands for the inter-layer interaction in the system and confirms the fact these NSs are not single-layered entities. To verify the few layers nature and estimate the number of layers we have performed the atomic force microscopy (AFM). The AFM topographical image in Figure 2e shows many small flakes of WSe_2. These flakes are comprised of an average height of 4-5 nm (Figure 2f), which corresponds to 5-6 monolayers.

Table S1: Transient fitting parameters of the all four excitonic features, as well as the prominent positive signal observed in the TA spectra.

Probe Wavelength (nm)	**τ_1 (ps)**	**τ_2 (ps)**	**τ_3 (ps)**	**τ_4 (ps)**
445	< 0.1 (+100 %)	0.78 (-63.6 %)	255 (-20.2 %)	> 1000 (-16.2 %)
530	< 0.1 (+100 %)	2.6 (+100 %)	55 (-51.7 %)	> 1000 (-48.3 %)
595	< 0.1 (+100 %)	2.4 (+100 %)	44.2 (-46.2 %)	> 1000 (-53.8 %)
630	1.5 (+100 %)	68 (-48.4 %)	> 1000 (-51.6 %)	-
747	< 0.1 (+100 %)	0.54 (-57.8 %)	171 (-25.9 %)	> 1000 (-16.3 %)

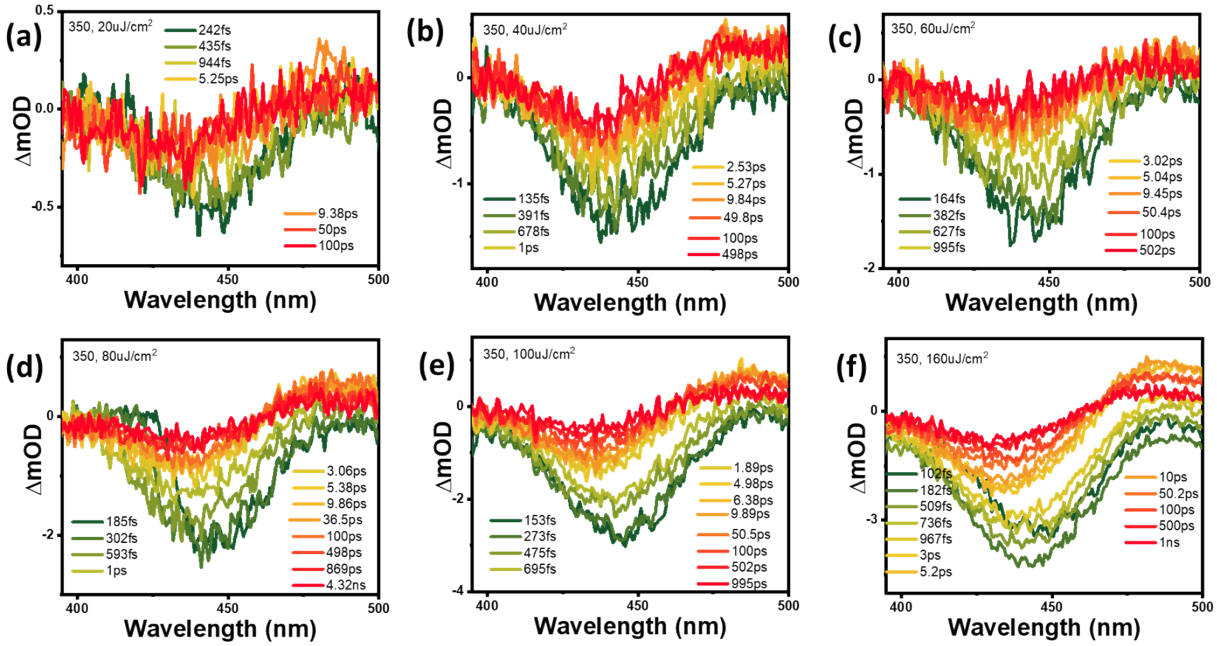

Figure S3: Transient absorption spectra of WSe_2 thin film monitoring in the UV-Vis region for D exciton, following 350 nm photoexcitation for **(a)** 20, **(b)** 40, **(c)** 60, **(d)** 80, **(e)** 100, and, **(f)** 160 μJ/cm^2 pump fluence.

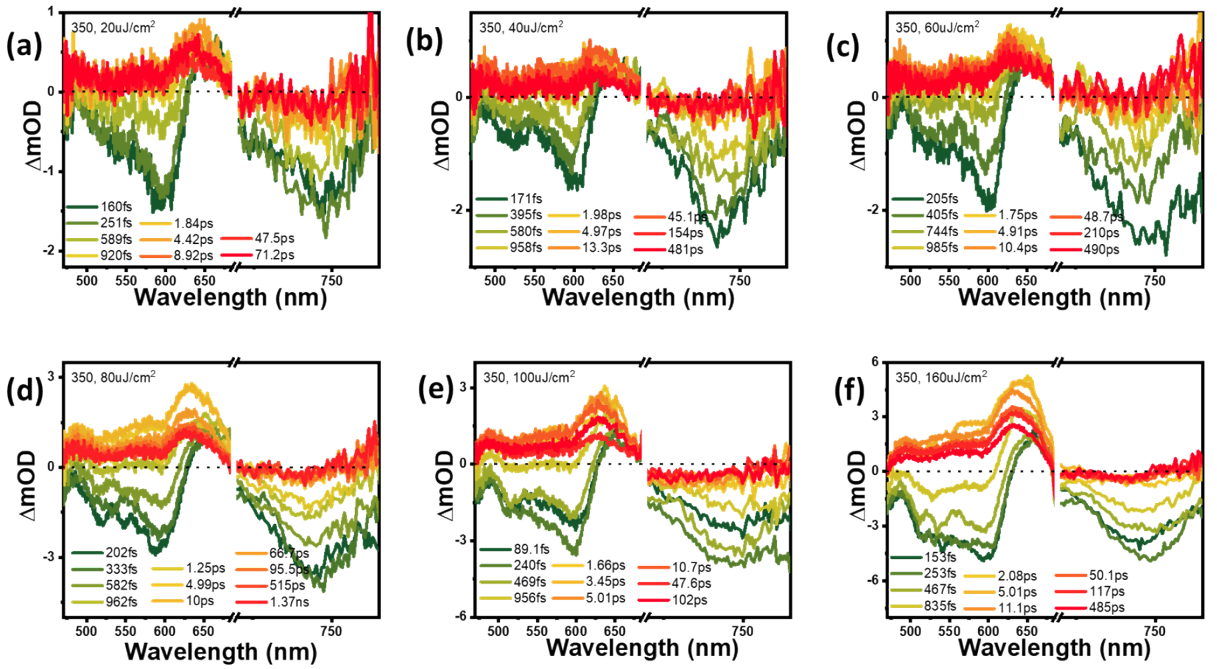

Figure S4: Transient absorption spectra of WSe_2 thin film monitoring in the Visible region for A, B, and C excitons, following 350 nm photoexcitation for **(a)** 20, **(b)** 40, **(c)** 60, **(d)** 80, **(e)** 100, and, **(f)** 160 μJ/cm^2 pump fluence.

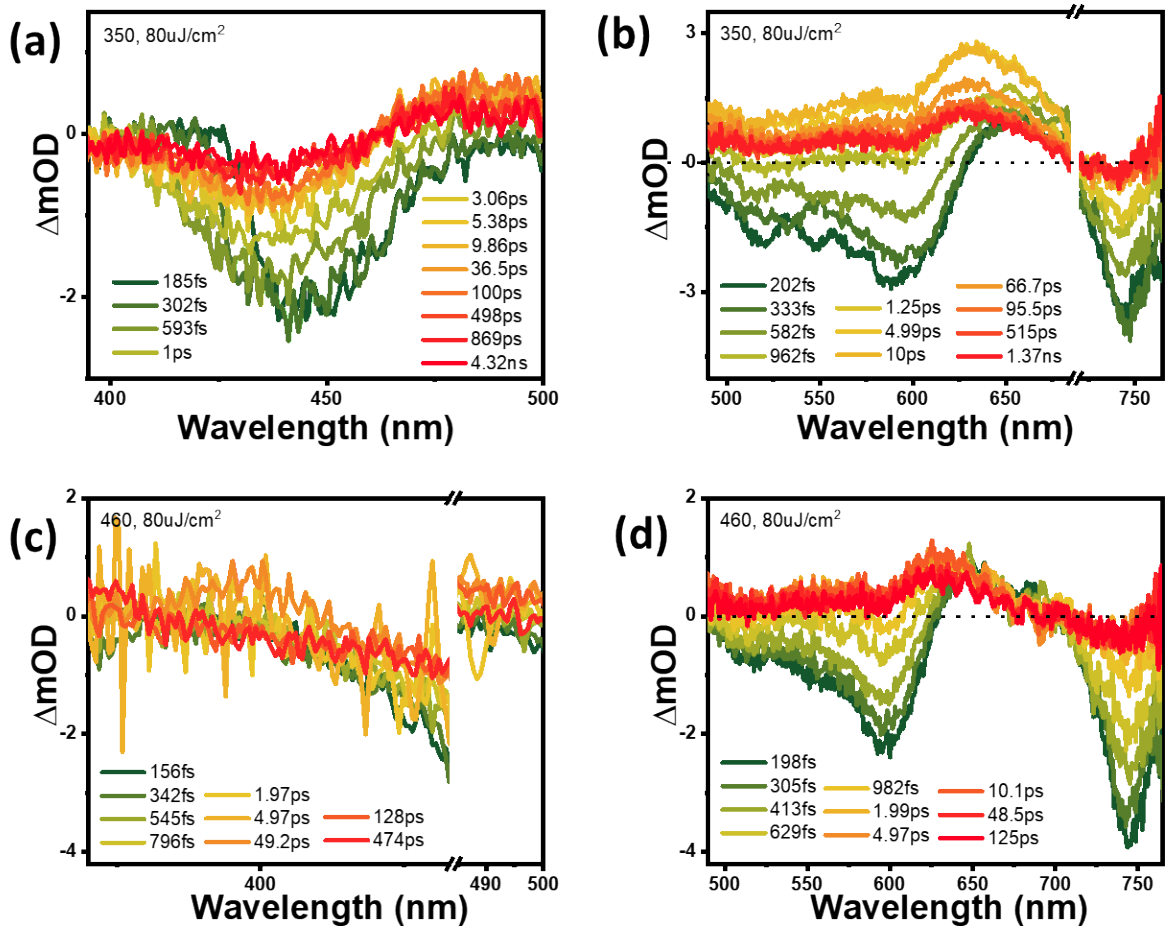

Figure S5: Transient absorption spectra of WSe_2 thin film monitoring in the UV-Vis region for D exciton and Visible region for A, B, C excitons, following 350 and 680 nm photoexcitation.

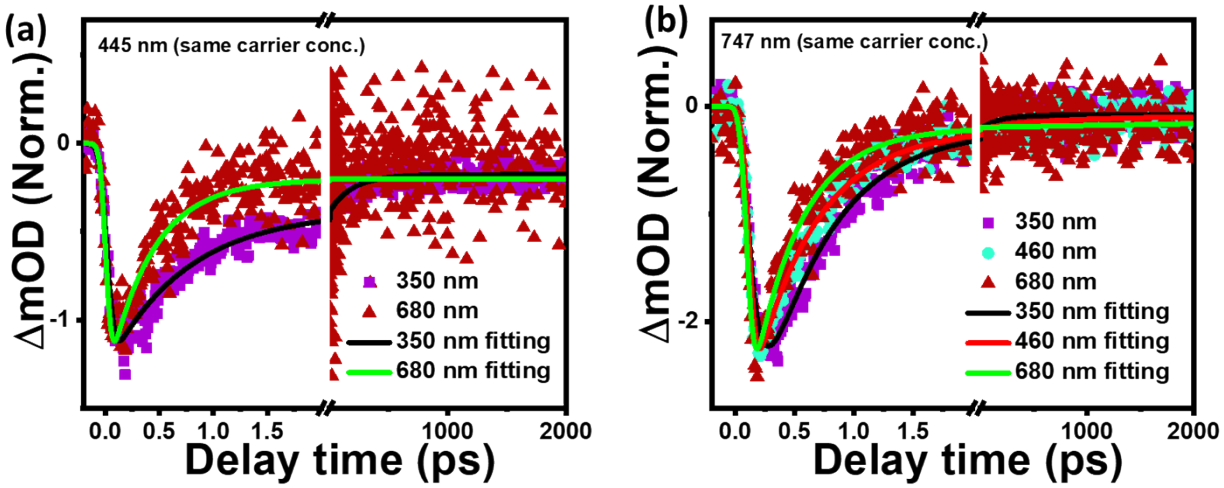

Figure S6: a) Normalized dynamics of D excitons, for 350 and 680 nm photoexcitation. **(d)** Normalized dynamics of A excitons, for 350, 460, and 680 nm photoexcitation.

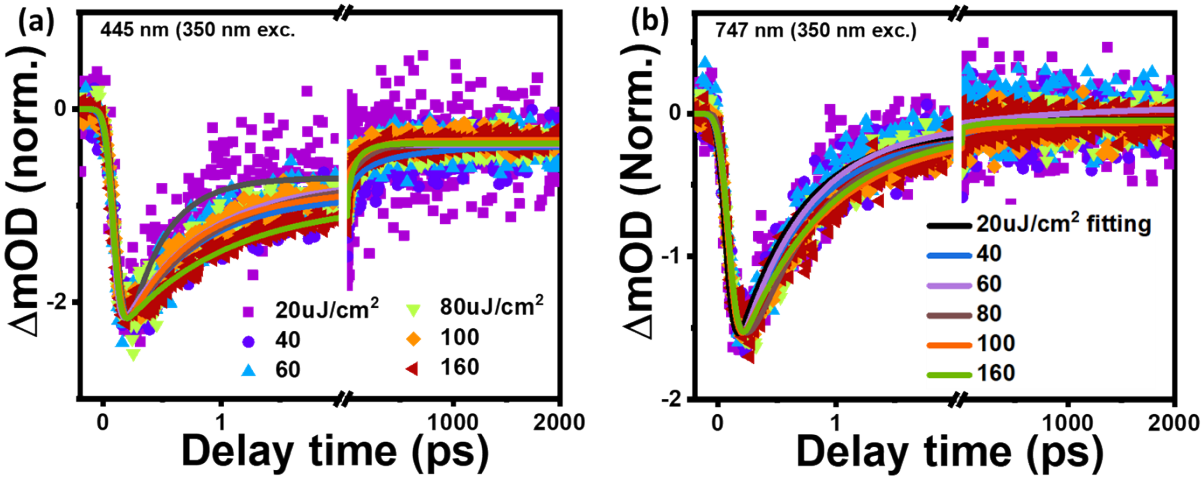

Figure S7: Normalized dynamic profiles of **(a)** D exciton and **(b)** A exciton, following 350 nm photoexcitation at room temperature for different pump fluence. The fluence range was maintained at 20-160 μJ/cm^2 in both the cases.

Table S2: Transient fitting parameters of D exciton at different pump fluence.

Pump fluence (μJ/cm^2)	**τ_1 (ps)**	**τ_2 (ps)**	**τ_3 (ps)**	**τ_4 (ps)**
20	< 0.1 (+100 %)	0.34 (-62.9 %)	126 (-19.1 %)	> 1000 (-18.1 %)
40	< 0.1 (+100 %)	0.52 (-54.2 %)	198 (-22.7 %)	> 1000 (-23.1 %)
60	< 0.1 (+100 %)	0.62 (-61.6 %)	200 (-21.3 %)	> 1000 (-17.1 %)
80	< 0.1 (+100 %)	0.78 (-63.6 %)	255 (-20.2 %)	> 1000 (-16.2 %)
100	< 0.1 (+100 %)	0.82 (-60.2 %)	276 (-25 %)	> 1000 (-14.8 %)
160	< 0.1 (+100 %)	0.94 (-53.2 %)	282 (-30.5 %)	> 1000 (-16.3 %)

Table S3: Transient fitting parameters of A exciton at different pump fluence.

Pump fluence ($\mu J/cm^2$)	**τ_1 (ps)**	**τ_2 (ps)**	**τ_3 (ps)**	**τ_4 (ps)**
20	< 0.1 (+100 %)	0.38 (-82.3 %)	210 (-15.0 %)	> 1000 (-2.7 %)
40	< 0.1 (+100 %)	0.42 (-81.0 %)	232 (-14.4 %)	> 1000 (-4.6 %)
60	< 0.1 (+100 %)	0.54 (-89.5 %)	250 (-9.7 %)	> 1000 (-0.8 %)
80	< 0.1 (+100 %)	0.54 (-85.0 %)	262 (-11.3 %)	> 1000 (-3.7 %)
100	< 0.1 (+100 %)	0.58 (-83.0 %)	270 (-12.0 %)	> 1000 (-5.0 %)
160	< 0.1 (+100 %)	0.62 (-83.0 %)	292 (-13.6 %)	> 1000 (-3.4 %)

Based on our previous study[5], we can ascribe three-time scales as inter-valley electron transfer (Γ-K for D and Λ-K for C), intra-valley thermalization in Λ and Λ-Γ indirect recombination, respectively. The first two processes would be significantly affected by the occurrence of Pauli-blocking for the electrons in the K and Λ valleys. In the following figure, we plotted the fitting parameters of these two processes at different excitation density. The fitting parameters of A excitons are also plotted for reference. We found that, the time constants associated with the D excitons are significantly influenced with the increment of pump energy (or excitation density). While these fitting parameters tend to get saturated in case of A excitons. Also, the effect of pump fluence is not identical for the time constants (τ_2 and τ_3) associated with the intervalley electron transfer and the intravalley thermalization process. The change in τ_2 is very significant throughout the applied fluence range. While τ_3 gets saturated in the higher range of pump fluence range. These observations essentially indicate toward the presence of Pauli blocking effect in the K-Λ region. Increased charge carrier density in this region induces Pauli blocking phenomena, which in turn hampers the intervalley electron transfer process from the Γ region. As we introduce more and more charge carrier in the system, this process gets slower. On the other hand, intravalley thermalization process would have little effect at higher pump fluence (≥ 80 $\mu J/cm^2$), as these states are already saturated with charge carriers. At the similar range of pump fluence, intervalley electron transfer rate is reduced dramatically.

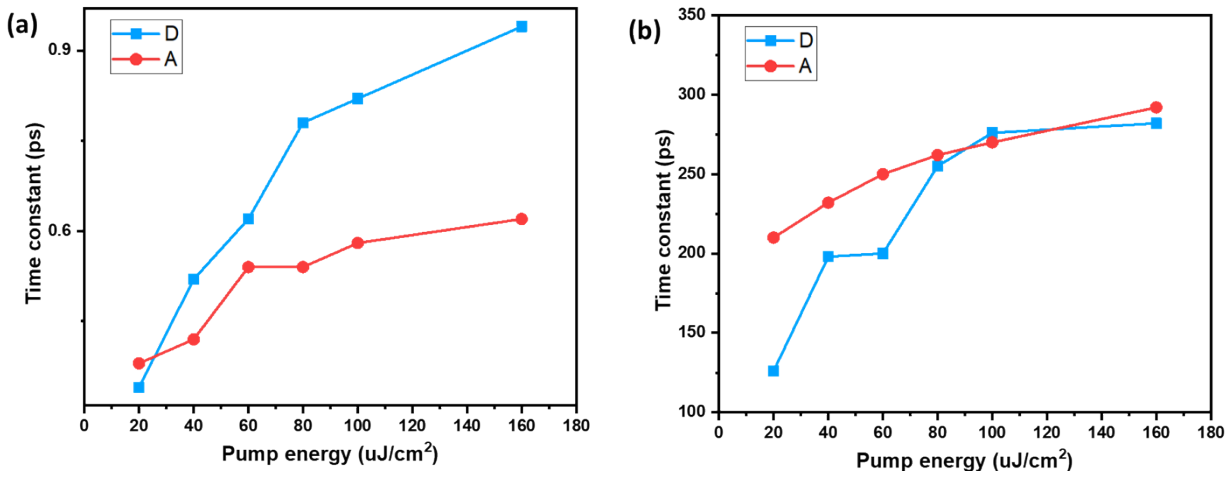

Figure S8: Plot of the fitting parameters **(a)** τ_2 and **(b)** τ_3 of A and D excitons, following 350 nm photoexcitation at room temperature for different pump fluence.

References:

1 H. Zeng, G.-B. Liu, J. Dai, Y. Yan, B. Zhu, R. He, L. Xie, S. Xu, X. Chen, W. Yao and X. Cui, *Sci Rep*, 2013, **3**, 1608.

2 E. del Corro, H. Terrones, A. Elias, C. Fantini, S. Feng, M. A. Nguyen, T. E. Mallouk, M. Terrones and M. A. Pimenta, *ACS Nano*, 2014, **8**, 9629–9635.

3 H. Terrones, E. Del Corro, S. Feng, J. M. Poumirol, D. Rhodes, D. Smirnov, N. R. Pradhan, Z. Lin, M. A. T. Nguyen, A. L. Elías, T. E. Mallouk, L. Balicas, M. A. Pimenta and M. Terrones, *Sci Rep*, 2014, **4**, 4215.

4 H. Sahin, S. Tongay, S. Horzum, W. Fan, J. Zhou, J. Li, J. Wu and F. M. Peeters, *Phys Rev B*, 2013, **87**, 165409.

5 T. Goswami, H. Bhatt, K. J. Babu, G. Kaur, N. Ghorai and H. N. Ghosh, *J Phys Chem Lett*, 2021, **12**, 6526–6534.